Item identification with a space-dependent model of neutron multiplicities and artificial neural networks

N.B. When citing this work, cite the original published paper.

(article starts on next page)

Item identification with a space-dependent model of neutron multiplicities and artificial neural networks

Senada Avdic [a], Victor Dykin [b], Stephen Croft [c], Imre Pázsit [b],*

[a] *Faculty of Science, Department of Physics, University of Tuzla, 75000 Tuzla, Bosnia and Herzegovina*
[b] *Division of Subatomic, High Energy and Plasma Physics, Chalmers University of Technology, SE–412 96, Göteborg, Sweden*
[c] *Lancaster University, Bailrigg, Lancaster, UK*

ARTICLE INFO

ABSTRACT

A method of calculating the neutron multiplicity rates (singles, doubles and triples rates), based on transport theory, was developed by us recently. The model treats the full 3-D spatial transport and multiplication of neutrons, accounting also for the shape of the item and the spatial distribution of the source, in one-speed theory. For a given item and its source distribution, the model can predict the multiplicity rates more precisely than the point model, on which traditional neutron multiplicity counting is based. However, so far it has not been investigated how the enhanced accuracy of the calculated multiplicity rates (i.e. the solution of the direct task) can be used to estimate the parameters of interest of the measurement item, primarily the fission rate (the solution of the inverse task). Unlike for the point model, the multiplicity rates under the extended scheme can only be given numerically, as solutions of integral transport equations, and hence an analytical inversion of the formulae is not possible. In this work it is investigated how machine learning methods, primarily the use of artificial neural networks, which only need numerical values of the solution of the direct task (the multiplicity rates), can be used for this purpose. It is shown that for numerical test items containing a mixture of ^{239}Pu and ^{240}Pu, the fraction of the latter varying between 4% and 25%, one can extract the masses of both isotopes from a properly trained network.

1. Introduction

Neutron multiplicity counting is a non-destructive method of determining the fission rate of a multiplying material [1–3]. The material usually consists of both fissile and fertile material, such as ^{239}Pu and ^{240}Pu as metal, or their oxides, plus possibly a matrix of non-fissile material, where here the ^{240}Pu plays the role of the source of spontaneous fission (SF) neutrons. The primary fission rate is the intensity of the spontaneous fission events, hence determining the fission rate amounts to determining the mass of the ^{240}Pu content of the item.

One has to add that in reality the SF rate is governed by a linear combination of the ^{238}Pu, ^{240}Pu and ^{242}Pu content, which is traditionally clumped together and described by an effective mass of ^{240}Pu. Also, fission can be induced in all Pu isotopes present, including ^{241}Pu. ^{241}Am, a decay product of ^{241}Pu can add to the (α, n) source term in oxides and impure metals. In the present demonstration of concept we simplify the item description for clarity by considering only ^{239}Pu and ^{240}Pu mixtures in pure metallic form, for which the (α, n) contribution is zero.

The fission rate is determined from the measured singles, doubles and triples rates (S, D and T rates, also commonly referred to as multiplicity rates), i.e. the rate of detecting in coincidence one, two and three neutrons emitted from the item. One can derive analytical expressions for these from a simplified model (the so-called point model) of the internal multiplication in the item. These formulae are derived such that the first three factorial moments of the number of neutrons leaving the sample due to a source event (spontaneous fission or (α, n) event) are first expressed by the lumped parameters of the item. The factorial moments are then easily converted to S, D and T rates through the source event intensity and the detector efficiency.

In the usual point model, similarly to the theory of the Feynman- and Rossi-alpha methods of determining the subcritical reactivity of a reactor core, the material is assumed to be homogeneous, and all neutrons have the same energy (one-speed model). The leakage of the neutrons from the finite sample (which does not appear in the Feynman- and Rossi-alpha methods) is described by a universal first collision probability leading to fission, which is the same for all neutrons of all generations in the chain. Spatial transport, and hence the scattering events, are completely disregarded. Only the fission reaction, and the multiplicities of the spontaneous and induced fission neutron multiplicities, or rather their first three factorial moments, are explicitly accounted for.

The point model is obviously a substantial simplification of the true physical processes. On the other hand, it has the strength which all lumped parameter models have in solving inverse tasks. Namely, even if it might not give an accurate description of the direct task, i.e. predicting the multiplicity rates for a given sample correctly, it has some definite advantages. Because it supplies a simple expression for the multiplicity rates, which contain only a very few global parameters, it is amenable to an analytical inversion, i.e. to express the sought sample parameters in terms of the measured multiplicity rates and known nuclear constants (fission neutron multiplicities). Further, experience shows that this inversion or unfolding procedure, perhaps surprisingly, is remarkably robust and reliable, in that the item fission rate is determined with a reasonably good accuracy, independently of the fine details of the item.

Nevertheless, despite the robustness, the simplifications represented by the point model will inevitably lead to an item specific systematic error, or bias, in determining the parameters of the item. Again, this is analogous to the Feynman- and Rossi-alpha methods [3], where it is known that a significant deviation in the system behaviour from point kinetics leads to a bias in the determination of the subcritical reactivity. This is only a conceptual comparison, since from the neutron physics point of view, the safeguards problem (deeply subcritical, neutronically thin systems with fast neutrons) and that of reactivity measurement (large, thermal systems close to criticality) differ significantly. To remedy the problems of the Feynman- and Rossi-alpha methods, corrections are usually applied. These corrections are not straightforward, since they only work if some a priori knowledge on the geometry and materials make-up of the system is available, hence they are not universally applicable, or require an unfolding procedure in which some extra parameters of the system beyond those of the lumped parameter method also need to be unfolded. The gain of introducing a more complete model of the system is therefore not granted.

Although the above problem has been studied extensively with regards to reactivity measurement methods, no similar studies have been conducted what regards the possible improvement of the point model-based multiplicity counting methods by introducing more realistic models (except possibly comparisons with Monte-Carlo predictions, or by the weighted point model [4]). Therefore, in recent work, we initiated the extension of the point model-based multiplicity counting to more realistic models [5–7]. We elaborated the stochastic theory of emission of neutrons from a finite item with a given geometry, using one-speed transport theory. At the beginning, similarly to the point model, fission was considered as the only reaction that the neutrons can undergo. Quantitative results were obtained for simple shapes, such as spheres, cylinders and shells, both with distributed neutron sources (which is the default assumption in nuclear safeguards tasks) as well as with point sources (as it was in the case of the measurements made on the Rocky Flats Shells during the MUSIC experimental campaign [8–11]).

Comparison of the calculated results with these latter measurements, made on items with known geometrical and material properties, as well as with known criticality data of pure ^{235}U and ^{239}Pu spheres, gave us the possibility to validate the extended model. It was found that in order to have a good agreement, scattering events had to be accounted for. Given the small energy loss and nearly isotropic angular distribution of the elastically scattered neutrons on heavy nuclei (assuming pure metallic items), elastic scattering could be included into the model, while still keeping its one-speed character. On the other hand, inclusion of inelastic scattering would require the extension of the model to energy-dependent cases and the handling of input data libraries. While work in this direction is already underway [12], in the works cited above the effect of inelastic scattering was estimated by an empirical way only, namely by a suitable choice of the neutron energy (which influences both the cross sections and the fission neutron multiplicities). This way, a reasonably good agreement was obtained between the measurements and calculations, as well as between the calculated and true critical sizes of pure ^{235}U and ^{239}Pu spheres.

Having reached this point, even if the extended model is not perfect, one can now investigate the question how this substantially more realistic model can be used for the unfolding of item parameters. This concerns both the elaboration of the unfolding procedure, as well as its mass assay accuracy. Since the factorial moments, and hence also the multiplicity rates can only be obtained numerically (through a collision number expansion solution of the corresponding integral equations), an analytical inversion is not possible. The most straightforward method appears to be the application of artificial neural networks (ANNs). In this procedure, first the model is used to generate a large set of training patterns, i.e. S, D and T rates, belonging to items of various sizes and isotopic compositions over ranges that likely to appear in practice. The trained network then receives a measured triplet of multiplicity rates (S, D and T) as input, from which it can unfold a few relevant parameters of the unknown item, as it will be discussed in Section 3.

The purpose of the present paper is to investigate the feasibility of such a procedure, together with its accuracy, and to make a first study of the conditions of its applicability. In Section 2, the principles of the space-dependent calculation of the multiplicities are briefly summarized, in comparison with the point model. Then the details of the use of the model to generate the training set as input to the ANN are discussed. In Section 3 the training and the test of the ANN are described. It is shown that within the assumptions and limitations of the model (mainly, its relying on some a priory knowledge on the item), the trained ANN can extract not only the mass of the ^{240}Pu, but also that of the ^{239}Pu directly from the measurement, thereby outperforming the point model not only in accuracy, but also in the range of applicability.

2. General principles

For the sake of completeness, the principles of both the point model and the space dependent model will be briefly summarized here. This is not only to make the paper self-contained, but it is also necessary in order to compare the advantages and disadvantages of the two approaches. And not the least, it is needed for the description of the unfolding method based on the space dependent model, which is the main subject of the paper.

2.1. The point model

From this point on, the description will be restricted to the case of pure metallic items, in which no (α, n) reactions take place, hence in the traditional expressions one has the ratio of (α, n) to spontaneous fission neutrons, $\alpha = 0$. This is not only for the sake of the simplification of the formalism, but also for intrinsic characteristics of the transport model-based sample identification, as will be elaborated on in the forthcoming. The case of $\alpha \neq 0$ requires special considerations, which will be discussed in a subsequent communication.

As is known, under these conditions the multiplicity rates S, D and T are expressed in terms of the factorial moments $\tilde{\nu}_i$, $i = 1, 2, 3$, of the number of neutrons emerging from the item following a source event (spontaneous fission) as

$$S = F \, \varepsilon \, \tilde{\nu}_1 \tag{1}$$

$$D = \frac{F \, \varepsilon^2 \, f_d}{2} \, \tilde{\nu}_2 \tag{2}$$

$$T = \frac{F \, \varepsilon^3 \, f_t}{6} \, \tilde{\nu}_3. \tag{3}$$

In the above, F is the spontaneous fission rate (to be determined), ε is the detector efficiency (counts per emergent neutrons, assumed to be known), and f_d and f_t are the doubles and triples gate factors, which account for the finite period of observation following every recorded neutron event (in the continuation assumed to be unity). Following the conventions used in most of our previous work, such as in [3], the tilde

in the $\tilde{v}_i$ indicates that these are the factorial moments of the number of neutrons emitted from the item generated by a *source* event (primary or initiating spontaneous fission), in order to distinguish them from the factorial moments of the neutrons emitted from the item for a *single* starting neutron (which will be needed in the next Section).

On their turn, the $\tilde{v}_i$ are given by

$$\tilde{v}_1 = \mathbf{M}\, v_{sf,1} \tag{4}$$

$$\tilde{v}_2 = \mathbf{M}^2 \left[v_{sf,2} + \left(\frac{\mathbf{M}-1}{v_{r,1}-1} \right) v_{sf,1}\, v_{r,2} \right] \tag{5}$$

$$\tilde{v}_3 = \mathbf{M}^3 \left[v_{sf,3} + \left(\frac{\mathbf{M}-1}{v_{r1}-1} \right) \left[3 v_{sf,2}\, v_{r,2} + v_{sf,1}\, v_{r,3} \right] \right.$$
$$\left. + 3 \left(\frac{\mathbf{M}-1}{v_{r1}-1} \right)^2 v_{sf,1}\, v_{r,2}^2 \right] \tag{6}$$

Here,

$$\mathbf{M} = \frac{1-\mathrm{p}}{1-\mathrm{p}\, v_{r,1}} \tag{7}$$

is the leakage multiplication, defined in terms of the (unknown) probability p that a neutron released into the item will induce fission, the $v_{r,i}$, $i = 1, 2, 3$ are the known factorial moments of the number of neutrons born in an induced fission in the fissionable isotope, and the $v_{sf,i}$ are the factorial moments of the number of neutrons emitted in a spontaneous fission event (which is the only primary source of neutrons in absence of (α, n) reactions), also known. In (7) we have also neglected parasitic capture mechanisms.

Naturally, one could have written the expressions for the S, D and T rates in a more compact form, by substituting Eqs (4)–(6) into (1)–(3), as was done e.g. in [5,13]. The equations here were kept separate on purpose, in order to have a better comparison with the similar expressions of the space-dependent model, where a compact form is not possible to give.

The unfolding of the unknown parameters F and $\mathbf{M}$ (and when relevant, the α factor), is achieved by first deriving and solving an algebraic equation for the leakage multiplication $\mathbf{M}$, and then substituting the solution to Eqs. (4) and (1) to express the fission rate. The general procedure is described in the literature [2,13,14]. Here we only write down the procedure for $\alpha = 0$, which is a special case of known α. Then, having only two unknowns, it is sufficient to use the S and D rates (this point will be returned on later). An equation of second order for $\mathbf{M}$ can be derived in the form

$$a + b\, \mathbf{M} + \mathbf{M}^2 = 0 \tag{8}$$

where the coefficients a and b are given as

$$a = -\frac{2\, D\, (v_{r,1}-1)}{S\, v_{r,2}}, \tag{9}$$

$$b = \frac{v_{sf,2}\,(v_{r,1}-1) - v_{sf,1}\, v_{r,2}}{v_{sf,1}\, v_{r,2}}, \tag{10}$$

after which the fission rate can be obtained from substituting the solution to (4) and (1).

A few comments are in order here, before turning to the space-dependent model, to facilitate the comparison of expected performance of the two models. The first is that in the point model, one does not need to be concerned with the shape of the item, since it cannot be taken into account explicitly. The effect of the geometry is represented by the fission probability p, which is an unknown of the procedure, hence one might expect that it will "adjust itself" to the actual geometry. Assuming a uniform (volume-averaged) fission probability for all generations of neutrons is of course an approximation, which will lead to a bias in the fission rate extracted. This bias may be different for the different geometries, as was discussed recently [5,6]. Nevertheless, it is a strength of the point model that its application is not bound to a given geometry of the item. This is in contrast to the case of the space-dependent model.

The second remark concerns the fact that the primary neutron source, whose fission rate is the most important parameter to be determined, and which supplies the effective mass of the ^{240}Pu component, is treated conceptually. Its spatial distribution, which certainly affects the multiplicity moments, is not specified. Again, this lacking knowledge is included in the fission probability parameter, which might compensate for this lacking information. More important, the fact that induced fission may take place in the non-fissile component, is traditionally completely neglected. The factorial moments $v_{r,i}$ are conventionally taken to be solely those of the fissile component, the ^{239}Pu, and no neutron reactions in the ^{240}Pu component are taken into account. This may be a good approximation for low ^{240}Pu content in the item, but it becomes increasingly worse with the increase of the ^{240}Pu content. As it will be seen in Sections 2 and 3, fission in both isotopes can be accounted for in the space-dependent model.

The last remark is that the identification procedure based on the point model can only determine the fission rate, and hence the mass, of the ^{240}Pu content of the item. There is no way that the more interesting ^{239}Pu mass could be extracted by the same non-destructive method. The point model only extracts the leakage multiplication, which is related to the mass of the fissile component in an indirect and unknown way. Hence the determination of the ^{239}Pu mass requires the laboratory determination of the ^{239}Pu/^{240}Pu ratio, which, on its turn, requires the application of destructive methods, or a different non-destructive method, usually high resolution gamma spectroscopy. As it will be seen in the forthcoming text, the identification procedure based on the space-dependent model has the potential to be able to extract the ^{239}Pu mass of the item, since it accounts for all reactions in the full isotopic content of the item.

2.2. The space-dependent model

The principles of this model, and quantitative results obtained from it, were published in a few recent papers [5–7]. In this model there are no lumped parameters, such as the fission probability or the leakage multiplication. Rather, the full geometry, and the possible reactions that the neutrons can undergo, are accounted for through a one-speed transport equation. In the first two papers, similarly to the point model, only induced fission in the fissile isotope was accounted for, and the source was also treated in a similar way, as a source of neutrons, but without taking the presence of the non-fissile component into account through neutron reactions. In the most recent publication [7], which aimed to yield results comparable with some present measurements made on the Rocky Flats Shells [8–11], the need to include the elastic scattering into the formalism arose. Elastic scattering could be included into the formalism in a relatively simple way, as it will be described below. The spontaneous fission neutron source (a small amount of ^{252}Cf in the cavity in the middle of the shell) was still accounted for in a conceptual way (no induced fission reactions in the ^{252}Cf were taken into account), which is a rather good approximation. However, since the Rocky Flats Shells have a composition of 93% ^{235}U and 7% ^{238}U, the model was extended to the case of using cross sections and multiplicities in a medium containing two isotopes.

The above formalism, which will be described concretely below, contains all ingredients which are necessary to calculate the multiplicity rates emerging from an item containing a mixture of ^{239}Pu and ^{240}Pu with a given weight percentage. It will be assumed that the item is homogeneous, which means that the source is uniformly distributed within the sample. In order to calculate the multiplicity rates, one has also to fix the geometry of the item. As mentioned before, neither the source distribution, nor the shape of the item is either necessary or possible to specify in the point model. These can and must be specified in the space-dependent model, which is both to its advantage and disadvantage. But for a class of measurement problems this may not be restrictive, and of course the point model and the extended model results can both be generalized for comparison.

Below the principles of the model will be specified for the case described above, i.e. a uniform mixture of two Pu isotopes according to a weight percentage for an item with spherical shape, with the inclusion of scattering. First we start with the inclusion of scattering in a material containing a single isotope. As described in [7], if one neglects the slight energy loss and slight anisotropy of the elastically scattered neutrons,[1] then one can interpret scattering as a fission event with one outgoing neutron. The procedure is completely analogous with how the effect of (α, n) neutrons can be combined with the number distribution of the spontaneous fission, to obtain the probability distribution, and hence the factorial moments, of the source emission event.[2]

Let us denote the induced fission and elastic scattering macroscopic cross sections with Σ_f and Σ_{el}, respectively, and introduce the total cross section Σ_T and the fractional contributions c_f and c_{el} of fission and scattering, respectively as[3]

$$\Sigma_T = \Sigma_f + \Sigma_{el}; \quad c_f \equiv \frac{\Sigma_f}{\Sigma_T}; \quad c_{el} \equiv \frac{\Sigma_{el}}{\Sigma_T} \tag{11}$$

Then, if f_k stands for the number distribution of the induced fission neutrons, with $\nu_{f,i}$ being its factorial moments, then the probability distribution $p_r(k)$ of the number of secondaries in a *reaction* will be given as

$$p_r(k) = c_f f_k + c_{el} \delta_{k,1} \tag{12}$$

and hence one has for the factorial moments $\nu_{r,i}$ of the number of secondaries as

$$\nu_{r,i} = c_f \nu_{f,i} + c_{el} \delta_{i,1} \tag{13}$$

Regarding a mixture of two isotopes, then one has to calculate first the fission and elastic scattering cross sections for the mixture. This is made by first calculating the fission, elastic scattering and total cross section of the mixture, and then applying Eqs. (11) and (13). In principle, this is a very simple task, if one knows the density of the compound and the weight fractions of the components. As is described in [7], this simply requires the application of the well-known formula

$$\Sigma_x^i = \sigma_x^i w_i \rho \frac{N_{Avo}}{M_i} \tag{14}$$

where x stands for the type of the reaction (fission or elastic scattering) and i for the nuclide index in question (239 for ^{239}Pu and 240 for ^{240}Pu), w_i is the weight fraction of the corresponding isotope, ρ is the density of the compound, σ is the microscopic cross section, and N_{Avo} stands for Avogadro's number. Once the fractional cross sections are found, they are simply added to represent the fission, elastic and total cross section of the mixture. The fission neutron multiplicities, and hence also the factorial moments thereof, will be weighted averages of the two isotopes, the weighting factors being the relative contributions of the individual fission cross sections to the total fission cross section of the compound [7]. The only problematic point here is that the density of Pu samples with different isotopic content is not available in general for an unknown item being assayed. We will return to this point later.

With these preliminaries, the calculation of the S, D and T rates in the space dependent model is performed as follows. Eqs. (1)–(3) remain the same, the difference is in the model representation and the consequent calculation of the factorial moments $\tilde{\nu}_i$. This will be described only very cursorily for spherical geometry, with the details of the derivation we refer to [5,12]. The starting point is the equation for the probability distribution $p(n\,|\,r, \mu)$ of the number of neutrons emitted

from the item by one single source neutron with co-ordinates (r, μ). By adding the probabilities of the mutually exclusive events of having or not having a first collision for the starting neutron to the system boundary, one has

$$p(n\,|\,r, \mu) = e^{-\ell(r, \mu)} \delta_{n,1} +$$
$$\int_0^{\ell(r,\mu)} ds\, e^{-s} \sum_0^\infty p_r(k) \sum_{n_1+n_2+\cdots+n_k=n} \int_{-1}^1 \frac{d\mu_1}{2} \frac{d\mu_2}{2} \cdots \frac{d\mu_k}{2} \times \tag{15}$$
$$p(n_1\,|\,r'(s), \mu_1)\, p(n_2\,|\,r'(s), \mu_2) \ldots p(n_k\,|\,r'(s), \mu_k).$$

In writing down (15), the radial coordinate is expressed in units of the mean free path $1/\Sigma_T$. Here $r'(s)$ is the radial position of the neutron at a distance s away from the starting point r along direction μ, and $l(r, \mu)$ is the distance, in optical units, to the boundary of the system from the radial position r in direction μ.[4] Introducing the generating function $g(z\,|\,r, \mu)$ of $p(n\,|\,r, \mu)$ in the usual way, one obtains the more compact equation

$$g(z\,|\,r, \mu) = z\, e^{-\ell(r, \mu)} + \int_0^{\ell(r,\mu)} ds\, e^{-s}\, q_r \big[g(z\,|\,r'(s)) \big]. \tag{16}$$

where $g(z\,|\,r)$ is the "scalar" (angularly integrated) generating function, q_r is the generating function of the number distribution of neutrons from a reaction, and $g(z\,|\,r'(s))$ here stands as its argument.

Eq. (16) shows similarities with the corresponding equation of the point model [1,3], except that it is an integral equation, not a pure algebraic equation. From (16) equations can be derived for the factorial moments of the emitted neutrons due to a single starting neutron, which are still integral equations, hence, in contrast to the point model, cannot be solved explicitly. These factorial moments, which are functions of the coordinates (r, μ) of the starting neutron, were denoted as $n(r, \mu)$, $m(r, \mu)$ and $w(r, \mu)$ in our previous work. We will quote only the equation for the first moment $\nu_1(r, \mu) \equiv n(r, \mu)$:

$$n(r, \mu) = e^{-\ell(r, \mu)} + \nu_{r,1} \int_0^{\ell(r,\mu)} ds\, e^{-s}\, n(r'(s)). \tag{17}$$

where $n(r'(s))$ is the angularly integrated first moment. As is always the case with backward type master equations, completely analogous equations can be derived for the second and third moments, with the only difference that the inhomogeneous part on the right hand side, $e^{-\ell(r, \mu)}$, will be replaced by functions of the lower order moments. These equations need to be solved numerically and sequentially, since the equations for the higher order moments contain the solutions of the lower order moments as the inhomogeneous part of the equation. The numerical solution can be conveniently obtained by a Neumann-series (collision number) expansion, which was used in our previous work.

In possession of the factorial moments of the number of neutrons leaving the sample due to one single starting neutron, one can easily calculate the factorial moments $\tilde{\nu}_i$ (denoted in the previous space-dependent works as N, M and W, respectively), which are needed in (1)–(3) to obtain the space-dependent multiplicity rates S, D and T. These are derived from an equation connecting the probability of the emission of a total number of neutrons by a spontaneous fission event in the system, integrated over the system, weighted with the spatial probability density $p_r(r)$ of the occurrence of the spontaneous fission source event. For this one needs also the number distribution $p_s(k)$ of the source emission, which for the cases treated here is the probability that in a spontaneous fission there will be k neutrons emitted. Here we only write down the equation for the generating function $G(z)$ of emitted neutron number distribution due to a source emission, relating it to the single neutron initiated scalar generating function, which reads as

$$G(z) = \int_V dr\, p_r(r)\, q_s\, [g(z\,|\,r)] = \frac{1}{V} \int_V dr\, q_s\, [g(z\,|\,r)], \tag{18}$$

---

[1] The anisotropy of the scattering can be trivially easily incorporated into the model, as described in [12]. It is neglected here for simplicity.

[2] Similarly, one can formally include capture as fission in which no neutrons are emitted.

[3] The fractional contributions c_i and c_{el} were denoted as α_s and β_s in [7]. The new notations c_f and c_{el} are introduced here because they feel more logical and are easier to identify.

[4] As in the case of the traditional point model development, we are ignoring encapsulation effects, which formally we can accommodate in the definition of the efficiency, unless the container is highly reflective.

where $q_s(z)$ is the generating function of $p_s(k)$. Usually, one can assume that the source is uniformly distributed within the item, which is expressed by the second equality. Without going into details, it is seen that the factorial moments $\tilde{v}_i$ of $G(z)$ can be easily obtained from those of the scalar single neutron induced generating function $g(z|\boldsymbol{r})$, i.e. from $n(r)$, $m(r)$ and $w(r)$, by a simple integration.

It has to be mentioned that the above formalism, using one-speed transport theory and isotropic scattering in the laboratory system, can only be used for pure metallic items. The presence of low-Z elements, such as O in Pu oxides or both H and O in the presence of moisture, will lead to significant energy loss of the neutrons and non-isotropic scattering. Inclusion of this aspect into the model, likewise the inclusion of inelastic scattering, necessitates the extension of the model to account for energy dependence. Given the simple analytical form of the scattering function of elastic scattering, this extension is conceptually very straightforward and work in this direction is already underway [12]. Introducing a new variable will of course increase the computational burden significantly, but this is only a technicality.

Extending the model for items containing Pu oxides will not affect the complexity of the unfolding process. This is because the Pu/O ratio is fixed, and hence no new unknown appears in the formulae. The presence of moisture, on the other hand, means the appearance of an unknown quantity of light materials (H_2O). The complexity of the calculation of the direct task (the multiplicities) is not affected, apart from the fact that calculations will have to be made for a larger set of variables, including a variable amount of moisture. On the other hand, in the inversion step, a new unknown, the quantity of the moisture, will also have to be unfolded. The sensitivity of the method for the neglection of the presence of a small amount of moisture, as well as the possibility of unfolding the unknown amount of moisture, will be investigated in future work.

One can now discuss the possibilities of unfolding item specific model parameters from the measured multiplicity rates based on the space-dependent model. It is seen that unlike in the point model, where no assumptions need to be made on the geometry of the sample and the spatial distribution of the source, in the space dependent model these need to be specified in order to obtain concrete quantitative values of the multiplicity rates. Once assumptions are made on these, the corresponding multiplicity rates can be calculated. In this paper, to demonstrate the approach for the first time, we restrict the studies to spherical geometry and a homogeneously distributed primary neutron source, but the model is capable of calculations to any other geometry or source distribution, as is was demonstrated in [6,7]. In particular, in [15], comparisons were made between spheres and cylinders of various aspect ratios. On the other hand, the space dependent model is more realistic than the point model not only due to the fact that it treats the spatial transport of the neutrons, but also because it takes into account the presence of the non-fissile component (here, ^{240}Pu), explicitly. More importantly, the parameters of the fissile component appear explicitly in the equations, which gives a chance to determine not only the mass of the spontaneous fission source component, but also of the fissile component; in other words, the isotopic grade of the Pu present.

Since there is no explicit inversion formula available for the space-dependent model, the only way is to numerically generate a multitude of solutions of the direct task, i.e. calculating the multiplicity rates for a large number of item parameters, i.e. size of the item and varying fractional weights of the two components, covering the domain of cases likely to occur in practice. Then the input parameters to the calculation are selected which yield the multiplicity rates closest to the measured ones. This is a multidimensional optimization problem, which can be effectively tackled by the use of artificial neural networks, ANNs. An investigation of the performance of an ANN-based inversion procedure will be performed in the next section.

3. The ANN model

Artificial Neural Networks (ANNs) as an advanced numerical approach are suitable for modelling nonlinear relationships. They can be applied in different systems such as image, voice and text recognition systems [16] as well as in nuclear reactor diagnostics and monitoring [17,18]. In nuclear safeguards, neutron and gamma multiplicity rates based on the point-model were used for determining sample parameters by the ANN approach [19,20]. Another recent application concerns the investigation of partial defects in spent nuclear fuel assemblies [21,22].

The generation of the training set, namely that of the S, D and T multiplicity rates was performed as follows. For a given case, the total mass of the item and the weight fraction of the ^{240}Pu component was selected. If the density of the compound was known, then this would determine all input parameters to the space-dependent calculation of the multiplicity rates. The density of the compound constitutes a slight problem, since it is not known for a large number of different weight fractions of ^{240}Pu. If it was granted that in the mixture of the two isotopes each would be present with its own specific density, then one could calculate the density ρ of the compound by the formula

$$\frac{1}{\rho} = \frac{1-w}{\rho_{239}} + \frac{w}{\rho_{240}} \tag{19}$$

where w is the weight fraction of the ^{240}Pu component. In general, however, one cannot count on this assumption being true. For instance, for the Rocky Flats Shells, consisting of 93% ^{235}U (18.811 g/cm^3) and 7% ^{238}U (19.052 g/cm^3) (data taken from [23]), Eq. (19) would yield a density of 18.827 g/cm^3, whereas the true density of the shells, given by [24], is 18.66 g/cm^3, i.e. less than that of any of the two components. In the calculations we used the density of 15.9 g/cm^3 for a delta phase of plutonium given by [25].

With this, given the total mass and the weight fraction of ^{240}Pu, everything is available for the space-dependent model to calculate the multiplicity rates S, D and T, as it would be for a full Monte Carlo calculation of ground truth. The macroscopic cross sections for the compound, both the fission, elastic scattering and total cross section, can be calculated from the microscopic cross sections, taken from the ENDF/B-VIII library, and using the partial fission and elastic scattering cross sections of the compound, the multiplicity rates can also be calculated using the data from [26]. All cross sections and fission neutron multiplicities were taken at 2 MeV. The physical size of the item is calculated from the weight and the density, and the radius of the sphere in optical units is calculated from the total cross section of the compound. The spontaneous fission rate is determined uniquely from the mass of the ^{240}Pu and the specific spontaneous fission rate of 479 fission/s/g.

The neutron multiplicity rates for a Pu metal sphere with the ^{240}Pu fraction between 4 and 25% and the sphere radius between 0.3 and 1.7 cm were used as the input data for the constructed ANNs. The selected range of the sphere radii is of practical interest for nuclear safeguards. Naturally, a similar investigation for a larger range of radii can also be easily made. Weapon grade plutonium contains less than 7% of ^{240}Pu, fuel grade plutonium contains 7%–18% of ^{240}Pu, whereas reactor grade plutonium contains over 18% of ^{240}Pu [27]. According to [28] the fraction of plutonium isotope ^{240}Pu of most pressurized-water-reactor spent fuel upon discharge would typically be of the order of 21 percent. The isotopic composition of MOX fuel for Light Water Reactors (LWRs) includes about 25% of ^{240}Pu when first loaded. Plutonium metal plate (referred to as PANN), which is used as fuel of the Zero Power Physics Reactor (ZPPR) at the Idaho National Laboratory (INL) [29] contains 95% of ^{239}Pu and 4.5% of ^{240}Pu by mass. A set of four ^{240}Pu scrap metal samples with mass of 6.6 g each and the ^{240}Pu fraction between 6.3 to 24.9% were measured using a standard neutron coincidence counter, i.e. Plutonium Scrap Multiplicity Counter (PSMC), at the Joint Research Center (JRC) laboratory, Ispra [30,31].
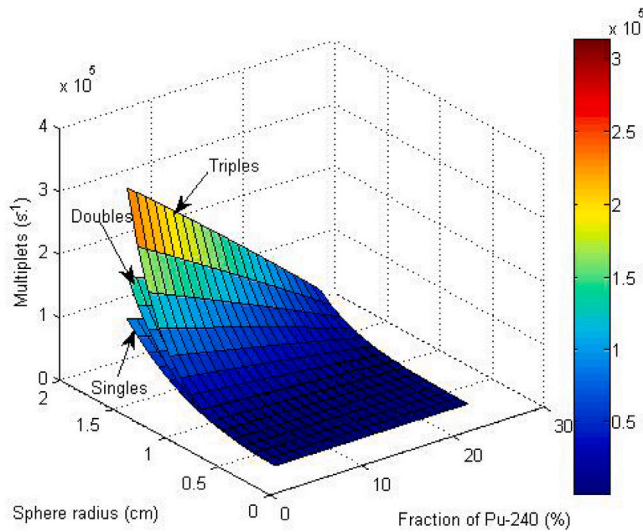
Fig. 1. Neutron multiplicity rates for a Pu metal sphere in the mass range between about 1.8 g and 327.2 g of plutonium.

Considering the data mentioned above, we selected the ^{240}Pu fraction between 4 and 25% for the initial ANN training data.

A training set consisting of the multiplicity rates according to Eqs. (86)–(88) in [5] was generated by assuming the alpha-ratio α (the ratio of the rate of random neutrons, that are mostly due to (α, n) reactions, to the rate of the average number of neutrons emitted from spontaneous fission [32]) is equal to zero, whereas the detection system efficiency, the gate utilization factors for doubles and triples counting were taken equal to unity [5]. For the investigation of the feasibility of the method, the actual value of the gate factors is irrelevant, because they affect the measurements and the corresponding simulations in the same way. In a concrete application, the simulations will have to be made by the proper values of the gate factors in the corresponding measurement.

The multiplicity rates S, D and T, calculated from the factorial moments, were used to generate input patterns for the training of a feed-forward backward-propagation network [33] with three inputs (originally the S, D, T rates for different values of the sphere radius and different values of the ^{240}Pu fraction; these inputs were modified later, see below); and the two outputs for the spontaneous fission rate F and the mass M of the ^{239}Pu content of the item[5] for each size of the sphere and each value of the ^{240}Pu fraction between 4 and 25%. The calculated multiplicity rates depending on the sphere radius and the ^{240}Pu fraction in the mass range between about 1.8 g and 327.2 g of plutonium are given in Fig. 1.

Given that in the absence of (α, n) neutrons, there are only two parameters to be determined (the spontaneous fission rate F and the mass M of the ^{239}Pu), in principle it would be sufficient to use only two measured quantities as the input of the ANN, namely the S and D rates, similarly to the analytic inversion of the point model for such a case, Eqs. (8)–(10). However, an ANN can very effectively utilize redundant information, represented here by the T rate, which is particularly useful in the case of possible uncertainties in the input data, which is always the case in practice. Indeed, as will be shown shortly, using the S, D and T rates as opposed to using the S and D rates only, improves both the convergence speed of the training and the accuracy of the unfolding of the two searched parameters F and M.

Another possibility would be to use the S, D and T rates to unfold, in addition to F and M, a third parameter, namely the detection efficiency ε. To this order one has to use an ANN with three input and three output nodes. This possibility was also investigated. However, it was found that the detection efficiency could not be determined with an acceptable accuracy, and in addition the accuracy of the unfolding of the other two parameters, F and M, also decreased noticeably. Just out of interest, we made then a conceptual test to unfold the detection efficiency with an ANN structure of three input nodes and one single output node, this latter yielding the detection efficiency ε. All three parameters (F M and ε) were varied during the training, but only ε was unfolded. In that case, the determination of ε was successful. However, since such a scenario lacks any practical relevance, this investigation will not be discussed any further, and in the continuation only results with unfolding of F and M with ANNs having three input and two output nodes will be reported.

As is the case when solving any multi-variable problem, especially in a purely numerical way with possible uncertainties in the input data, a pre-requisite of a successful and accurate solution is that the dependent variables (in our case the S, D and T values) are sufficiently sensitive functions of the independent variables (here, F and M).[6] In pattern recognition parlance, this means that the selected feature parameters should be sensitive functions of the input patterns. In a linear system of differential equations, this can be decided from the determinant of the characteristic equation. No such possibility is available for the present case, where only a highly implicit numerical relationship exists between the input and output data.

However, one can check the suitability of the selected features (the inputs of the indirect task, such as S, D and T, or their various combinations) by calculating the correlation coefficients between them for a set of randomly chosen input variables F and M of the direct task, by a bootstrap procedure. This means selecting fixed values of the input data F and M, and then varying their values as if adding a "random noise" to these input parameters. The outputs S, D and T are then calculated for each random value of the inputs, and the correlation coefficient is calculated. A strong correlation between these data, which serve as the input of the ANN, is an indication of an expected deteriorated performance of the process of extracting the F and M data.

The accuracy of identification with the ANN depends on how sensitive the results are to the input parameters of the ANN (the multiplicities). In the search of the most sensitive set of input data, we tested both the pure S, D and T multiplicity rates as the input data to the ANN, as well as some combinations such as S, D/S and T/S and S, D/S and T/D. Fig. 2 shows histograms of the correlation coefficients obtained after 1000 times bootstrap sampling of input vectors with added 3% by magnitude of a random noise drawn from the normal distribution. The correlation coefficient between inputs such as S, D/S and T/S can be reduced from 0.99 (S, D) to 0.81 for the second configuration (S, D/S) and from 0.98 (S, T) to 0.83 for the third configuration (S, T/S). Accordingly, as Fig. 3 shows, the target mass of the ^{239}Pu and fission rate was recovered with significantly better accuracy (smaller deviation or error of the identification) for the ANN input set S, D/S and T/D than for the original input set S, D, T. Fig. 4 shows the effect of the input data configuration on the ANN unfolding results by a comparison between the cases of three versus two input data. It can be seen that the relative deviations of the unfolded results from the target values for both parameters such as the mass of the ^{239}Pu content and the spontaneous fission rate are smaller for the configuration with three inputs than with those with two inputs.

In the unfolding calculations, we have used a typical feed-forward ANN consisting of interconnected neurons, with an input layer, one or more hidden layers (one layer for the case with "clean" input data and two layers for "noisy" input data), and an output layer. Fig. 5 shows the structure of the case with one hidden layer.

---

[5] The mass M of the ^{239}Pu content of the item is not to be mixed up with the leakage multiplication $\mathbf{M}$ of the point model, Eq. (7).

[6] Note that F and M are the input and S, D and T are the output of the *direct* task, i.e. the calculation of the multiplicity moments from the material
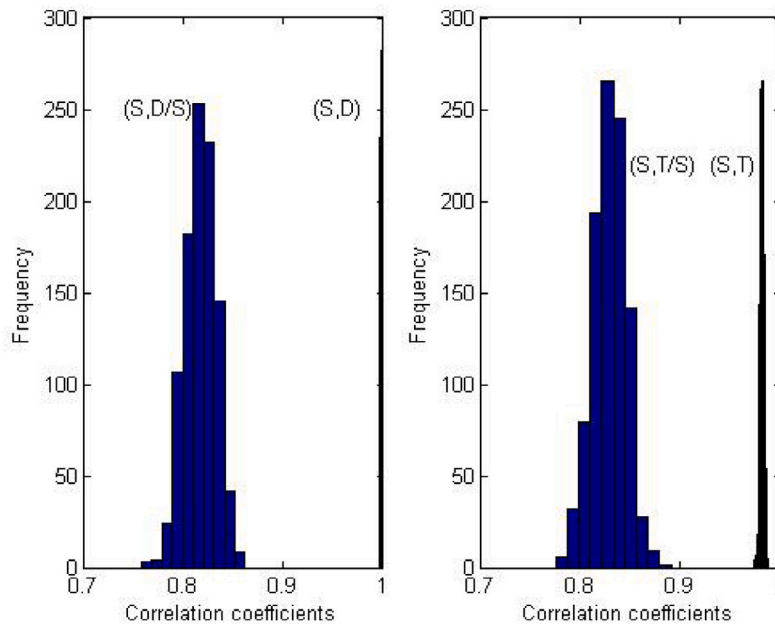
Fig. 2. Histograms of the correlation coefficients obtained by bootstrap sampling of the input data with random noise.
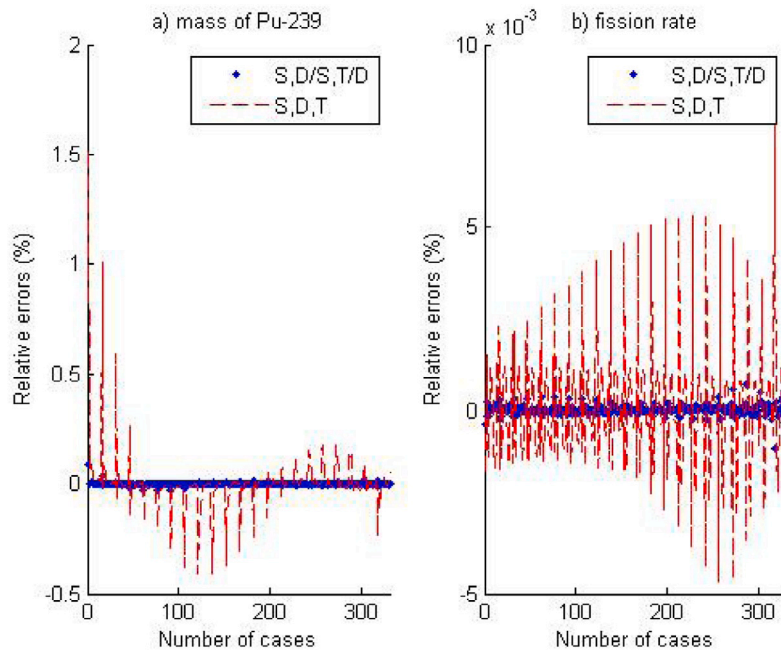

Fig. 3. The unfolding results for the input data set S, D/S T/S compared to the S, D, T input configuration.

4. Results

4.1. Fission rate and ^{239}Pu mass unfolding from the multiplicity rates without noise

In order to properly tune the constructed ANN for the problem studied, sets of inputs (the multiplicities calculated from the factorial moments) and outputs (the mass of ^{239}Pu and the fission rate) are used for learning the ANN relationship. The number of neurons in the input layer corresponds to the number of input features, the number

in the output layer is equal to the output size, whereas the number of neurons in hidden layers needs to be tuned in order to optimize the algorithm performance. We used the Neural Net Fitting application [33] to create a feed-forward network with one hidden layer with 20 nodes determined on the basis of the k-fold cross validation analysis.

K-fold cross-validation is a process used to estimate the accuracy of an ANN model. It is a common practice to randomly divide data into 10-folds or subsets of roughly equal size. In each run, one of the folds is used for validation and the remaining folds for training. The process is repeated k times so that each of the k subsets is used once for validation. The estimate of the ANN model accuracy was taken as the average value of a performance function in each run. The data set of the constructed ANN includes 330 cases for the input multiplicity rates depending on the sphere radius in the range between 0.3 and
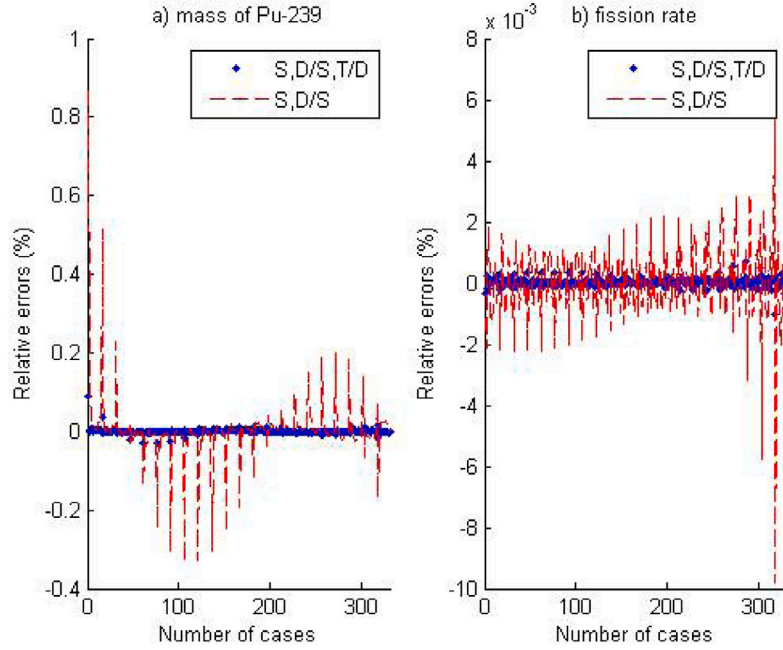
---

and geometry data of the item. The ANN solves the *inverse* task, hence it takes the S, D and T as input, and supplies the F and M as its output.

Fig. 4. The effect of the input data configuration on the accuracy of the ANN unfolding results.
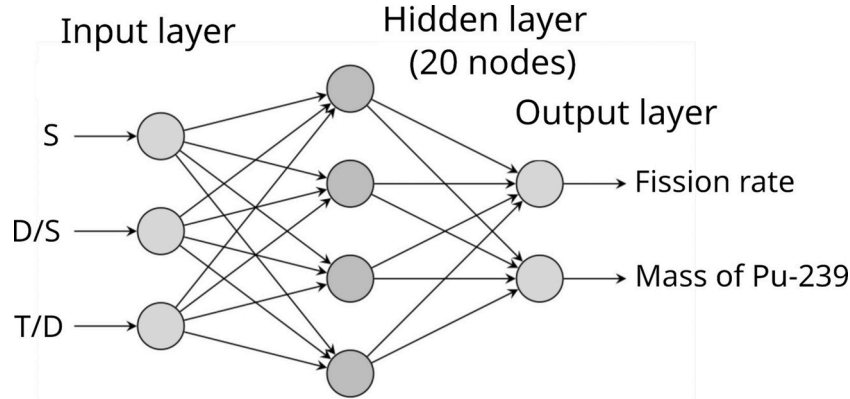

Fig. 5. A typical feed-forward ANN used in the unfolding calculations.

1.7 cm with a step of 0.1 cm and the ^{240}Pu fraction between 4 and 25 wt% with a step of 1 wt%. The input data were split randomly into training (231 cases, i.e. 70%), validation (50 cases, i.e. about 15%), and test (49 cases, i.e. about 15%) sets. Bayesian regularization was applied via the network training function `trainbr` to produce a network that generalizes well.

The trained ANN was tested to determine the fission rate and the mass of ^{239}Pu of an unknown item. The difference between the recovered value by the ANN approach and the true (known) value indicates the inaccuracy of the unfolding method. This inaccuracy is different for each fold, and is random in its character. For simplicity, the deviation between the true value and the one recovered by the ANN, expressing the inaccuracy of an individual identification, will be termed as "error" or "errors" in the tables and figures, and the expressions "error", "deviation" and "inaccuracy" will be used interchangeably in the text and the captions. The maximum, minimum, mean and standard deviation of the relative errors obtained for the whole set of the input data (training, validation and test) used with the trained network are given in Table 1. Histograms of the relative deviations between the target and ANN values for the ^{239}Pu mass and the fission rate for the input data without noise are presented in Fig. 6. Table 1 and Fig. 6 demonstrate that the ^{239}Pu mass and the fission rate were unfolded with good precision in the test phase.

Table 1
Relative errors of the ANN outputs compared to the target values for the input data without noise.

Relative error (%)	^{239}Pu mass	Fission rate
Maximum	0.081	0.0077
Minimum	−0.0378	−0.0088
Mean	8.14e−05	3.02e−05
Standard deviation	0.0068	0.0018

4.2. Fission rate and ^{239}Pu mass unfolding from the multiplicity rates with added random noise

Since measurement data inevitably contain statistical uncertainties, in order to simulate more realistic input data, we added a random noise to all three neutron multiplicity rates S, D and T at a level of 3% in magnitude independently drawn from a normal distribution. The constructed network is somewhat more complex than the previous one and it includes two hidden layers with 35 and 15 nodes. Fig. 7 shows histograms of the relative errors, whereas the relative errors of the unfolded parameters are given in Table 2. The Figure and the Table show that the fission rate can be unfolded with a relative error less than
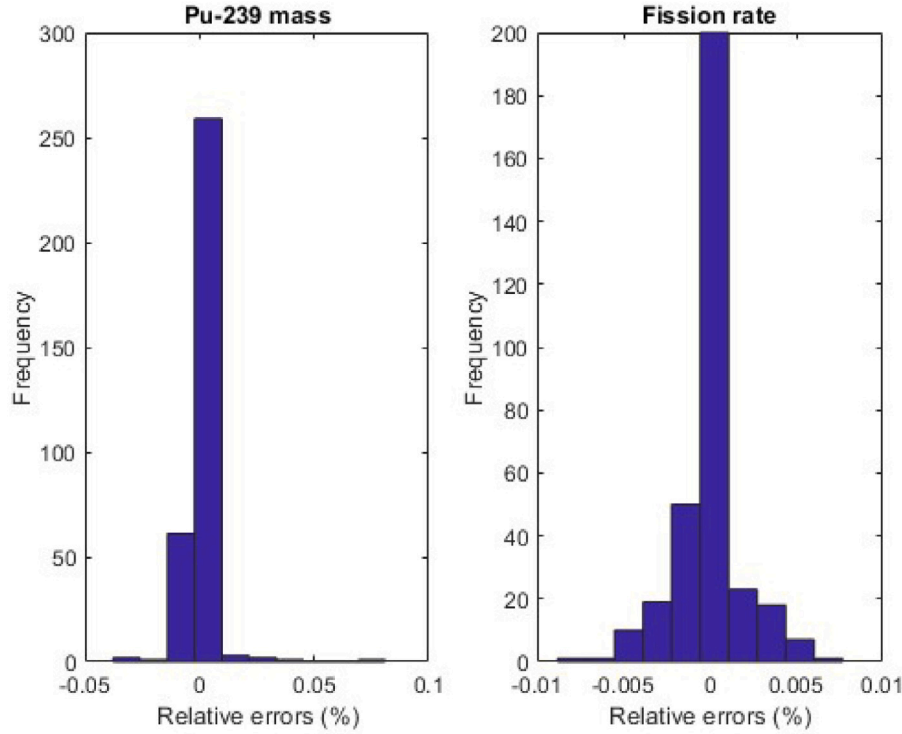
Fig. 6. Relative deviation between the target assay parameters and ANN values for the ^{239}Pu mass and the fission rate for the input data without noise in the input data.

Table 2
Relative errors of the ANN outputs compared to the target values for the input data with added random noise at a level of 3% of the magnitudes of the individual multiplicity rates.

Relative error (%)	^{239}Pu mass	Fission rate (F)
Maximum	3.95	0.3
Minimum	−4.15	−0.21
Mean	−0.008	−9.0e−04
Standard deviation	0.612	0.083

Table 3
Relative errors of the ANN outputs compared to the target values for the input data with added random noise.

Relative error (%)	^{239}Pu mass	Fission rate (F)
Maximum	0.59	0.013
Minimum	−1.04	−0.012
Mean	−0.007	−1.46e−04
Standard deviation	0.123	0.0042

about 0.3% whereas the ^{239}Pu mass can be evaluated with the relative error less than about 4.2%. In addition, we tested the ANN response for the input data with a random noise at a level of 5% added separately to the S, D, T rates (combinations: $(S + noise, D, T)$, $(S, D + noise, T)$ and $(S, D, T + noise)$) and to all of them in the combination $(S + noise, D + noise, T + noise)$. In all the combinations, the fission rate could be unfolded with a relative error less than 1%.

4.3. Fission rate and ^{239}Pu mass unfolding from the multiplicity rates with setting the standard deviations of added random noise to specific values

The S, D, T multiplicity rates for weapons-grade metal samples ("PM" samples) with the masses in the range of 10–20 g and about 4.5% of a ^{240}Pu content for two of the items and about 8.5% of a ^{240}Pu content for the third item were measured at the Joint Research Centre in Ispra [34]. The standard errors for the measured multiplicity rates S, D and T were 0.5, 0.5 and 1.1%, respectively. Guided by this experimental study, we have added random noise to the input data setting the standard deviations of added noise to given values for the measured S, D and T rates. The constructed ANN includes two hidden layers with 35 and 15 nodes. Histograms of the relative errors between the target and ANN responses for the ^{239}Pu mass and the fission rate for the input data with added noise are presented in Fig. 8, whereas the maximum, minimum, mean and standard deviation of the relative errors are given in Table 3.

5. Conclusions

The ANN approach was implemented to unfold a few parameters (the fission rate and the ^{239}Pu fraction) of an unknown plutonium item in the mass range between 1.8 g and 327.2 g. It was demonstrated that the constructed ANNs are suitable to unfold the fission rate as the most important parameter (relating to the ^{240}Pu mass) of interest in nuclear safeguards with high accuracy for the clean multiplicity rates and for the more realistic input data with added random noise even for the sample with a few grams of plutonium. In other words, it has been demonstrated that the ANN is a potential alternative to analytical methods when a more sophisticated interpretational model is adopted and analytical methods are not possible. The ANN unfolding results were obtained for the input data with a high spatial resolution (step of 0.1 cm) as well as for a high ^{240}Pu fraction resolution of 1%. It can be expected that the accuracy of the unfolded parameters can be improved in the wider range of the plutonium sample mass with the more pronounced differences between the neutron multiplicity rates.

The results of the current study showed how to extract the "correct" fissile mass of an unknown sample from the calculated neutron multiplicity rates based on the newly developed space dependent model and by using machine learning methods, i.e. by applying the ANN approach. The extended model is simpler and faster than a full Monte Carlo simulation, and is commensurate with the few observable (S, D, T) experimental data. The ANN approach is of course general and can be applied to any training set (experimental or MC simulated).
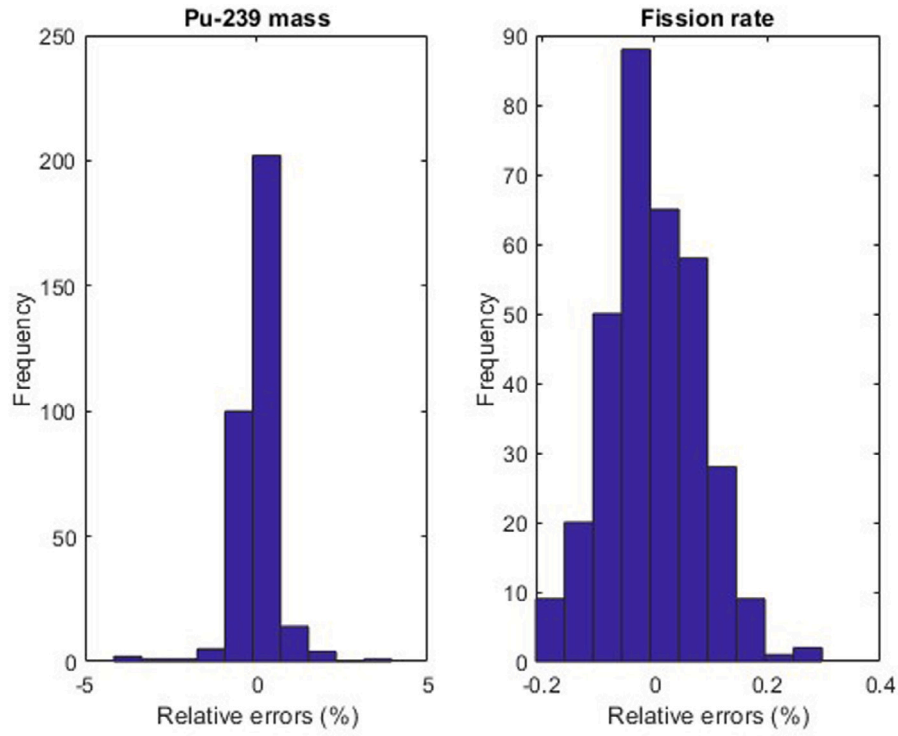
Fig. 7. Relative deviation between the target and ANN values for the ^{239}Pu mass and the fission rate with added random noise at a level of 3% of the magnitudes of the individual multiplicity rates.
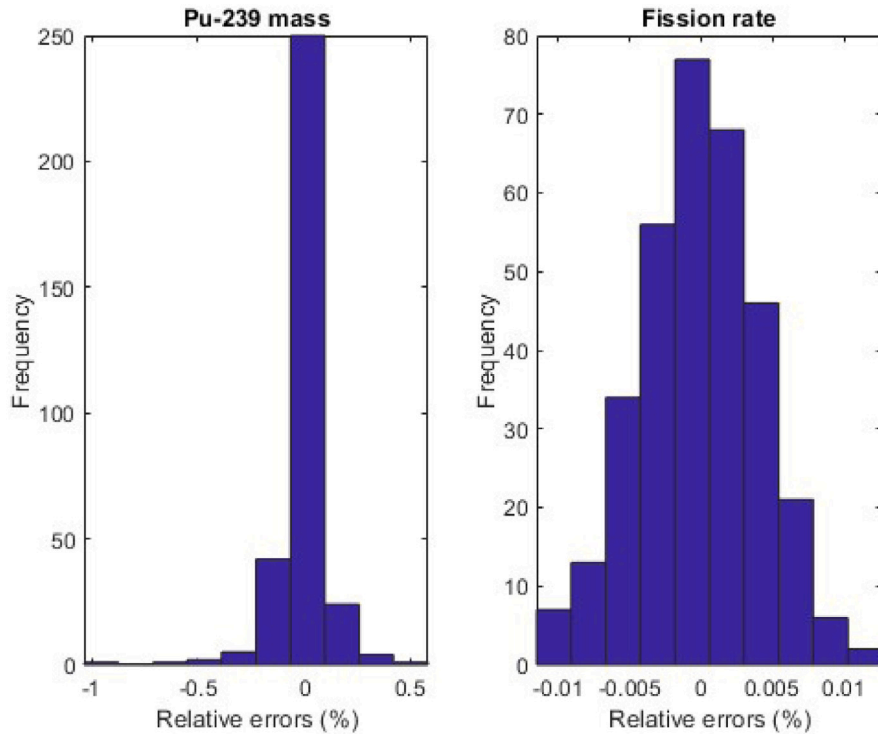

Fig. 8. Relative deviation between the target and ANN values for the ^{239}Pu mass and the fission rate with the added noise.

Declaration of competing interest

The authors declare that they have no known competing financial interests or personal relationships that could have appeared to influence the work reported in this paper.

Data availability

Data will be made available on request.

Acknowledgements

References

[1] K. Böhnel, The effect of multiplication on the quantitative determination of spontaneously fissioning isotopes by neutron correlation analysis, Nucl. Sci. Eng. 90 (1985) 75–82.

[2] N. Ensslin, W.C. Harker, M.S. Krick, D.G. Langner, M.M. Pickrell, J.E. Stewart, Application Guide to Neutron Multiplicity Counting, Los Alamos Report LA-13422-M, 1998.

[3] I. Pázsit, Neutron Fluctuations: A Treatise on the Physics of Branching Processes, Elsevier, New York, 2008.

[4] S. Croft, E. Alvarez, P.M.J. Chard, R. McElroy, S. Philips, An alternative perspective on the weighted point model for passive neutron multiplicity counting, in: Proc. 48th INMM Annual Meeting, Paper A130, 8-12 2007, Tucson, Arizona, 2007.

[5] I. Pázsit, L. Pál, Multiplicity theory beyond the point model, Ann. Nucl. Energy 154 (2021) 108119, http://dx.doi.org/10.1016/j.anucene.2020.108119, URL https://www.sciencedirect.com/science/article/pii/S030645492030815X.

[6] I. Pázsit, V. Dykin, Transport calculations of the multiplicity moments for cylinders, Nucl. Sci. Eng. 196 (2022) 235–249.

[7] I. Pázsit, V. Dykin, F. Darby, Space-dependent calculation of the multiplicity moments for shells with the inclusion of scattering, Nucl. Sci. Eng. (2023) 1–17, URL http://dx.doi.org/10.1080/00295639.2023.2178249.

[8] F. Darby, M. Hua, J. Hutchinson, G. McKenzie, R. Weldon, J. Lamproe, S. Pozzi, Examination of new theory for neutron multiplicity counting of non-point-like sources of special nuclear material, in: Proceedings of INMM & ESARDA Joint Virtual Annual Meeting, 2021.

[9] F.B. Darby, J.D. Hutchinson, M.Y. Hua, R.A. Weldon, G.E. McKenzie, J.R. Lamproe, S.A. Pozzi, Comparison of neutron-multiplicity-counting estimates with trans-stilbene, EJ-309, and He-3 detection systems, Trans. Amer. Nucl. Soc. 125 (1) (2021) http://dx.doi.org/10.13182/T125-36636.

[10] A. McSpaden, T. Cutler, J. Hutchinson, W. Myers, G. McKenzie, J. Goda, R. Sanchez, MUSIC: a critical and subcritical experiment measuring highly enriched uranium shells, France, 2019, iNIS Reference Number: 52011546.

[11] A.T. McSpaden, G.E. McKenzie, R.G. Sanchez, Progress Update on the MUSIC Critical Benchmark, Tech. Rep. LA-UR-22-26184, Los Alamos National Lab. (LANL), Los Alamos, NM (United States), 2022, URL https://www.osti.gov/biblio/1897647.

[12] I. Pázsit, V. Dykin, S. Avdic, Transport calculation of the multiplicity moments with energy dependence and anisotropic scattering, in: Proc. M & C 2023 - the International Conference on Mathematics and Computational Methods Applied to Nuclear Science and Engineering, Niagara Falls, Ontario, Canada, 2023.

[13] I. Pázsit, A. Enqvist, L. Pál, A note on the multiplicity expressions in nuclear safeguards, Nucl. Instrum. Methods A 603 (2009) 541–544.

[14] I. Pázsit, L. Pál, Multiplicity counting from fission detector signals, in: Proc. INMM Annual Meeting, Paper A499, Atlanta GA, 2016.

[15] V. Dykin, I. Pázsit, Geometry effects in the transport calculations of the multiplicity moments, in: Trans. Am. Nucl. Soc. 125, P. 754, November 30 - December 3 2021, Washington D.C, 2021.

[16] A. Jain, J. Mao, K. Mohiuddin, Artificial neural networks: A tutorial, Computer 29 (1996) 3144, http://dx.doi.org/10.1109/2.485891.

[17] I. Pázsit, M. Kitamura, The role of neural networks in reactor diagnostics and control, in: Advances in Nuclear Science and Technology, Vol. 24, Springer, US, Boston, MA, 1996, pp. 95–130.

[18] I. Pázsit, N. Garis, P. Lindén, Application of neural networks in reactor diagnostics and monitoring, in: D. Ruan (Ed.), Springer Series Studies in Fuzziness and Soft Computing, in: Fuzzy Systems and Soft Computing in Nuclear Engineering, vol. 38, 2000, pp. 258–284.

[19] A. Enqvist, I. Pázsit, S. Avdic, Sample characterization using both neutron and gamma multiplicities, Nucl. Instrum. Methods Phys. Res. A 615 (2010) 62–69.

[20] I. Pázsit, A. Enqvist, S. Avdic, Combined use of neutron and gamma multiplicities for determining sample parameters, in: International Conference on Mathematics, Computational Methods and Reactor Physics, Saratoga Springs, New York, 2009.

[21] M. Al-Dbissi, Developments Toward a Novel Methodology for Spent Nuclear Fuel Verification (Licentiate Thesis), Department of Physics, Chalmers University of Technology, Göteborg, 2022.

[22] M. Al-Dbissi, R. Rossa, A. Borella, I. Pázsit, P. Vinai, Identification of diversions in spent PWR fuel assemblies by PDET signatures using artificial neural networks (ANNs), Ann. Nucl. Energy 193 (2023) 110005.

[23] Mathematica, Version 13.2, Inc. Wolfram Research, Champaign, IL, 2022, URL https://www.wolfram.com/wolfram-alpha-notebook-edition.

[24] R. Sanchez, T. Grove, M. White, Measure the Fission Neutron Spectrum using Threshold Activation Detectors, Tech. Rep. LA-UR-11-07069, Los Alamos National Laboratory, 2006.

[25] G. Miloshevsky, A. Hassanein, Multiplicity correlation between neutrons and gamma-rays emitted from snm and non-snm sources, Nucl. Inst. Methods Phys. Res. B 342 (2015) 277–285.

[26] J.M. Verbeke, C. Hagman, D. Wright, Simulation of Neutron and Gamma Ray Emission from Fission and Photofission, Tech. Rep. UCRL-AR-228518, Lawrence Livermore National Laboratory, 2010.

[27] J. Green, Plutonium grades and nuclear weapons, 2007, online; updated September 10, 2007. URL https://www.foe.org.au/anti-nuclear/issues/nfc/power-weapons/rgpu.

[28] M. Carson, F. von Hippel, E. Lyman, Explosive properties of reactor-grade plutonium, Sci. Glob. Secur. 17 (2009) 170–185.

[29] A. Di Fulvio, T. Shin, T. Jordan, M. Sosa, S. Clarke, D. Chichester, S. Pozzi, Passive assay of plutonium metal plates using a fast-neutron multiplicity counter, Nucl. Instrum. Methods Phys. Res. A 855 (2017) 92–101.

[30] C. Dubi, S. Croft, A. Favalli, A. Ocherashvili, B. Pedersen, Estimating the mass variance in neutron multiplicity counting—a comparison of approaches, Nucl. Instrum. Methods Phys. Res. A 875 (2017) 125–131.

[31] J. Dolan, M. Flaska, A. Poitrasson-Riviere, A. Enqvist, P. Peerani, D. Chichester, S. Pozzi, Plutonium measurements with a fast-neutron multiplicity counter for nuclear safeguards applications, Nucl. Instrum. Methods Phys. Res. A 763 (2014) 565–574.

[32] S. Croft, A. Favalli, D. Hauck, D. Henzlova, P. Santi, Feynman variance-to-mean in the context of passive neutron coincidence counting, Nucl. Instrum. Methods Phys. Res. A 686 (2012) 136–144.

[33] MATLAB, Version (R2022a), The MathWorks Inc., Natick, Massachusetts, 2022.

[34] M. Gottsche, Reducing Neutron Multiplicity Counting Bias for Plutonium Warhead Authentication (Ph.D. thesis), Department of Physics, Universit at Hamburg, Hamburg, 2015.